BioFactors

WILEY

RESEARCH ARTICLE OPEN ACCESS

Optimizing Alternating Current Electrical Stimulation Parameters to Enhance Osteoblasts Differentiation

Jesús Bocio-Núñez[1,2] | Mª. José Montoya-García[3,4] | Mª. Ángeles Vázquez-Gámez[3,4] | Daniel Martín[5,6] | Pedro Chacón[7,8] | Miguel Ángel Rico[1,3] | Miguel Ángel Colmenero[1] | Alberto Yufera[5,6] | Mercè Giner[2,4]

[1]UGC Medicina Interna, Hospital Universitario Virgen Macarena, Seville, Spain | [2]Dpto. Citología e Histología Normal y Patológica, Universidad de Sevilla, Seville, Spain | [3]Dpto de Medicina, Universidad de Sevilla, Seville, Spain | [4]Instituto de Biomedicina de Sevilla (IBIS), Seville, Spain | [5]Instituto de Microelectrónica de Sevilla – Universidad de Sevilla (IMSE-US), Seville, Spain | [6]Dpto. Tecnología Electrónica, Universidad de Sevilla, Seville, Spain | [7]Departamento de Ciencias de la Salud y Biomédicas, Universidad Loyola Andalucía, Seville, Spain | [8]Laboratorio de Inmunología y Alergia-FISEVI, UGC de Alergología, Hospital Universitario Virgen Macarena, Seville, Spain

Correspondence: Mª. José Montoya-García (pmontoya@us.es)

Received: 30 October 2025 | **Revised:** 2 March 2026 | **Accepted:** 24 March 2026

Keywords: alternating current | electric-stimulation | MC3T3-E1 | osteoblasts | tissue engineering

ABSTRACT

Electrical stimulation (ES) has emerged as a promising technique in the field of bioengineering and biomedicine, particularly in bone regeneration and cell differentiation. ES using alternating current (AC) is based on the periodic reversal of current direction, which generates oscillating electric fields. The application of an electric field has effects on cell growth and differentiation, as well as on morphology and migration. This study aimed to explore the effect of applying AC electrostimulation within the proliferation, differentiation, and morphology process of osteoblastic cells. The electrical stimulation signals were daily applied for 3 h during 14 days. Different frequencies were tested (1 Hz, 10 Hz, 100 Hz, and 1 kHz), with amplitudes of 125, 250, 500, 750, 1000, and 1500 mV/mm. Cell viability was estimated using the AlamarBlue, and MC3T3-E1 differentiation levels were evaluated through alkaline phosphatase (ALP) activity. *RUNX2*, *OSX*, *ALP*, *OPG*, and *RANKL* gene expression was assessed by RT-PCR. Morphological analysis was performed through cell transfection followed by immunofluorescence. Statistical analysis was conducted by SPSS.23 and graphs generated through Graph-pad. Viability and ALP activity were optimal at 10 Hz. Once the frequency was defined, *RUNX2*, *OSX*, *ALP*, *OPG*, and *RANKL* gene expression revealed an increase in the differentiation and osteogenic activity levels at 10 Hz and 500–750 mV/mm. As well as, morphological studies showed an increase in the area, pseudopodia length, and numbers at 500 mV 10 Hz conditions. The optimal ES condition to differentiate MC3T3-E1 cells is 10 Hz 500–750 mV/mm. Electrostimulation has emerged as a promising technique in the field of bioengineering and biomedicine, particularly in bone regeneration and cell early maturation.

1 | Introduction

Bone regeneration therapy is essential for accelerating fracture repair, enhancing implant integration, and treating diseases that impair bone formation. Among the different strategies, electrostimulation (ES) stands out as a non-invasive approach that promotes osteoblast proliferation and differentiation, thereby facilitating the formation of new bone tissue. Electrical stimulation or electrostimulation is a technique based on the application of electrical currents to cells, mimicking the

Abbreviations: AC, alternating current; ALP, alkaline phosphatase; DAC, digital to analogue converter; ECM, extracellular matrix; ES, electrical stimulation; MSC, mesenchymal stem cells; OCN, osteocalcin; OPG, osteoprotegerina; OSX, transcription factor; RANKL, ligand for the RANK receptor; RUNX2, RUNX transcription factor family.

physiological currents, to guide cellular and tissue responses. The electrical signal applied is defined by adjusting parameters such as frequency, amplitude, and duration of the electrical signal [1].

Among the different electrostimulation methods, alternating current (AC) is particularly remarkable. AC electrostimulation is based on the periodic reversal of current direction, which generates oscillating electric fields [1]. It has been shown that, at a cellular level, the application of ES can affect the electrical environment of cells, thereby modifying ion channels, cytoskeleton reorganization, lipid rafts, membrane potential, and intracellular signaling pathways [1]. Furthermore, it is known that the application of an electric field has effects on cell growth and differentiation, as well as on morphology and migration [2]. ES has shown significant potential in tissue engineering and regeneration in diverse fields, such as dermatology and the nervous system, where it has been reported that it induces skin regeneration [3], neurite outgrowth, and synaptic plasticity [4].

The first attempt at using ES in the bone tissue field treating bone fractures was provided by Mollon and colleagues in 2008 [5]. Under physiological conditions, bone has an electronegative matrix. After an external factor such as bone overload or the presence of a fracture, this bone area experiences an increase in its electronegativity, where electrons and anions are accumulated, generating an ionic flow directed toward the damaged area [6]. The application of ES modifies this dynamic, intensifying the electronegativity and stimulating the attraction of osteogenic cells, accelerating bone regeneration [7].

Specifically, the effect of ES on osteoblasts has demonstrated an improvement in osteoblast function as well as the induction of osteogenic differentiation and maturation [8–10]. Osteoblastic differentiation is regulated, among other levels, in particular at the transcriptional level by transcription factors. RUNX2, a member of the RUNX transcription factor family, is crucial in embryonic skeletal development, in the early stages of mesenchymal stem cells (MSC) differentiation into pre-osteoblasts, osteoblastic differentiation, and for maintaining osteoblastic functions themselves [11, 12]. Its expression peaks in immature osteoblasts and decreases as cells differentiate, highlighting its fundamental role in early stages of osteoblastic differentiation [13]. Other osteoblast-specific transcription factor is osterix (OSX), encoded by the *SP7* gene. It plays a crucial role in the intermediate stages of maturation, also regulating the activity of functional osteoblasts and their subsequent differentiation into osteocytes [14, 15]. During maturation process, osteoblast increases alkaline phosphatase (ALP) synthesis protein. Subsequently, mineralization of the extracellular matrix (ECM) occurs through the expression of several osteoblastogenic marker genes such as osteocalcin (*OCN*), along with the continuous expression of *ALP* [16, 17].

At the molecular level, the RANK/RANKL/OPG system is essential for osteoclastic migration and activation. The RANKL protein acts as a ligand for the RANK receptor; its binding induces osteoclastic differentiation and inhibits osteoclast apoptosis. Furthermore, RANKL inhibits osteogenesis by causing β-catenin degradation and impeding its synthesis [18]. On the other hand, osteoprotegerin (OPG), a soluble protein with high affinity for RANKL, binds to it, preventing its interaction with RANK, thereby inhibiting bone resorption. Osteoblasts are the main source of OPG in bone [19]. Therefore, the RANKL/OPG ratio informs us about the amount of bone to be reabsorbed [20].

While several electrostimulation systems have been described in the literature, this study introduces and applies a novel, previously described system [21] to explore the effect of applying AC electrical stimulation within proliferation, early differentiation, and morphology process of osteoblastic cells MC3T3-E1.

2 | Experimental Procedures

2.1 | Materials

Phosphate-buffered saline (PBS), alpha-Minimum Essential Medium (α-MEM), OptiMEM medium, penicillin and streptomycin, GlutaMAX I, amphotericin-B, trypsin–EDTA, AlamarBlue Cell Viability Reagent, Tryzol, Superscript III first-strand synthesis system, Lipofectamine, and 4′,6-diamidino-2-phenylindole (DAPI) containing mounting medium were purchased from Thermofisher Invitrogen (San Diego, CA, USA). Heat-inactivated foetal bovine serum was from Capricorn (Ebsdorfergrund, Germany) and trypan Blue Stain from BioWhittaker-Lonza (Verviers, Belgium). β-glycerophosphate, ascorbic acid, dexamethasone, and all reagents of biochemical and molecular biology studies were purchased from MERK Sigma-Aldrich (Madrid, Spain).

2.2 | Experimental Electrostimulation Setup

The electrostimulation system was previously described by Martin et al. [22]. It included a signal generation circuit, a bed for holding cell culture plates, and a printed circuit board (PCB) for connections. The system generates ES signals using the digital to analogue converter (DAC) inside a Nucleo-STM32L4 microcontroller development board (STMicroelectronics, Geneva, Switzerland). These signals are later adapted and modulated by a set of amplifiers in differential and inverting configurations (OPAx228 Texas Instruments, Texas, USA). This system generates biphasic voltage squared ES signals, with amplitudes ranging from 125 mV to 1500 mV, and frequencies from 1 Hz to 1 kHz. Up to four 8W10E+ cell culture plates (Applied Biophysics, Troy, USA) were used, each with 8 wells and two sets of 20 interdigitated gold electrodes (250 μm diameter, 1 mm apart). These plates ensured uniform electric fields, with weaker lines at 90° and stronger ones at 45° and 135°. The PCB connected the plates to the signal circuit via 9 connectors and a pin header for interfacing.

2.3 | Cell Line Culture and Electrical Stimulation Protocol

The mouse preosteoblast cell line MC3T3-E1 (subclone 4, ATCC CRL-2593) was obtained from American Type Culture Collection (Manassas, VA, USA). Cells were cultured in complete growth medium (α-MEM containing 10% FBS, 2 mM GlutaMAX I, 100 units/

mL penicillin, 100 μg/mL streptomycin, and 2.5 μg/mL amphotericin-B) and kept in an incubator at 37°C[2]. After 72 h of culture, the medium was replaced with osteogenic medium (complete growth medium with supplements, i.e., 50 μg/mL ascorbic acid, 10 mM β-glycerophosphate and 10 nM dexamethasone). Cells were then cultured for 4, 7, and 14 days, being medium replaced three times per week. The electrical stimulation signals were daily applied for 3 h. For AC, different frequencies were tested (1 Hz, 10 Hz, 100 Hz, and 1 kHz), with amplitudes of 125, 250, 500, 750, 1000, and 1500 mV/mm. The waveform used was a biphasic square wave with a 50% duty cycle, as described in Martin et al. [22]. In all our experiments, three biological replicates in two independent experiments were analyzed for each day of the study in each defined voltage and frequency. in standard humidified atmosphere of 95% relative humidity (RH) and 5% CO. Subsequently, the cells were maintained with medium changes every other day and subcultured with trypsin–EDTA at 70%–80% confluence. Then cells were collected by centrifugation and viable ones counted using the trypan blue exclusion test. They were seeded in complete growth medium at 175,000 cells/cm.

2.4 | Cell Viability Assay

Cell viability was estimated using the AlamarBlue, according to the manufacturer's recommendations. Briefly, cell culture medium was removed from culture plates and replaced by 300 μL AlamarBlue mixture containing 10% AlamarBlue stock solution and 90% cell culture medium and incubated at 37°C for 120 min. Following incubation, three 50 μL replicates of the aliquots were transferred from each sample into a clear 96 well plate. A sample control (media plus AlamarBlue reagent) was required on this assay. Absorbance readings were taken using an Infinity 200 Pro microplate reader (TECAN, Switzerland), at 570 nm excitation and 600 nm emission.

2.5 | Alkaline Phosphatase (ALP) Activity Determination

MC3T3-E1 differentiation levels were evaluated through alkaline phosphatase (ALP) activity, using the Alkaline Phosphatase Assay Kit Colorimetric (Abcam ab83369, Abcam, Cambridge, UK). The assay was performed according to the manufacturer's protocol on the cell culture supernatant of control cells or cells subjected to electrical stimulation under different voltages and frequency conditions at 4, 7, 10, and 14 days of electrostimulation, in triplicate. Osteoblasts actively release this enzyme into the extracellular environment through matrix vesicles during the differentiation and mineralization process. While the experiment progressed, supernatants were collected and stored at −80°C until further use. The absorbance at 405 nm of 4-nitrophenol was measured using an Infinity 200 Pro microplate reader. Data were expressed as U/mL of pNPP (para-Nitrophenylphosphate).

2.6 | Gene Expression Analysis

Total RNA was isolated from MC3T3-E1 using Trizol reagent and further purified using the RNeasy mini kit (Qiagen, CA, USA) including a DNAse I treatment. cDNA was prepared from 1 μg total RNA using 500 ng random hexamers (Promega, WI, USA), 10 mM dNTPs (Promega), 40 U of RNase inhibitor RNasinPlus (Promega) and Superscript III first-strand synthesis system. Quantitative PCR was performed on the StepOne system (Applied Biosystems, Invitrogen) using FastStart Universal SYBR Green master (Rox) (Roche, France) and the specific primers showed in Table S1. Relative expression levels were calculated using the $2^{-\Delta\Delta CT}$ method and the housekeeping gene rRNA18S for normalization.

2.7 | Expression Vector, Cell Transfection and Immunofluorescence (IF)

The pmCherry vector was obtained from Takara Bio Company (CA, USA). After 9 or 13 days, culture medium was removed and replaced by a mixture containing 0.6 μg of plasmid and 2 μL of Lipofectamine in OptiMEM medium. After 3 h incubation, cells were washed and cultured in osteogenic medium for another 15 h. Cells were then fixed and analyzed by IF.

To determine cell proliferation, morphology and cell differentiation, IF was performed on MC3T3-E1 cells after 14 days of electrical stimulation. Cells were fixed with 4% paraformaldehyde for 15 min, permeabilized for 15 min at room temperature with 0.5% Triton X-100 in PBS and immediately blocked for 1 h with 1% bovine serum albumin in PBT (0.1% Triton X-100 in PBS). After blocking, the corresponding primary antibodies were added: rabbit anti-mCherry at 1:500 dilution (Abcam, Cambrigge, UK) in blocking solution and incubated for 1 h. After washing with PBT, the secondary antibodies (donkey Cy3 AffiniPure anti-Rabbit (H+L) (Jackson InmunoResearch, Cambridge, UK) at 1:500 dilution in blocking solution) were added and incubated for an additional hour. Plates containing PBS-washed cells were then mounted onto glass slides with DAPI-containing mounting medium.

2.8 | Cell Proliferation Counting and Morphometric and Cell Differentiation Analysis

Images of 40 random fields per condition or 40 mCherry$^+$ in three biological replicates were analyzed for each day of the study in each defined voltage at 10 Hz. This analysis was acquired digitally using a 20X objective (Olympus BX50, PA, USA). The samples were coded and randomized before microscope visualization. For the cell proliferation estimation, the number of DAPI-stained cells per field was counted using the Cell Counter plugin in ImageJ software. For the morphometric analysis, cell area, number of pseudophilopodia and maximal and media lenght of pseudophilodia of mCherry$^+$cells were analyzed by Image J software. Pixel scale calibration is set up for each image analysis (1 μm = 12 pixels).

A comprehensive overview of the experimental procedures employed in this study is shown in Figure 1.

2.9 | Statistical Analysis

Statistical analyses were carried out in SPSS 23.0 (IBM, Spain) and SigmaPlot 12.0 (Grafiti LLC, CA, USA). Data normality was

verified with the Shapiro–Wilk test, and all variables satisfied the assumption of normal distribution. Comparisons between independent groups were performed with Student's *t*-test (two groups) or one-way ANOVA (three or more groups); significant ANOVA results were followed by Tukey's post hoc test. Time-course measurements of ALP activity at 4, 7, 10, and 14 days were analyzed using paired *t*-tests. The impact of voltage and/or frequency on ALP activity was evaluated with a mixed-factor (two-way) ANOVA, incorporating the Greenhouse–Geisser correction. Effect sizes were expressed as partial eta-squared (ηp^2). All data are presented as mean ± standard error of the mean (SEM). Statistical significance was defined as $p < 0.05$ ($^*p < 0.05$; $^{**}p < 0.01$; $^{***}p < 0.001$). Each experiment was performed in at least triplicate.

3 | Results

Our initial approach consisted of systematically testing different combinations of frequencies and voltages to identify the most appropriate experimental settings to promote osteoblastic differentiation in MC3T3-E1 cells. Cell viability and ALP activity, both acknowledged as indicators of osteoblastic function, were employed as primary selection criteria. Once the optimal conditions were established, all subsequent experiments (gene expression analysis, morphometric and cell differentiation analysis) were conducted exclusively under these preselected parameters.

3.1 | Cell Viability

During the cell viability analysis in cell line MC3T3-E1 under AC stimulation, variations were observed depending on frequency and voltage applied (Figure 2). At lower voltages (125, 250, and 500 mV), the 100 Hz condition was the only one associated with a reduction in viability below 80% ($p < 0.001$). In contrast, at higher voltages (750, 1000, and 1500 mV), this effect was observed exclusively at 1 kHz. Conversely, the 1 Hz condition displayed a more stable response across all tested voltages, with minimal changes in viability. Notably, the 10 Hz condition exhibited a distinct profile: regardless of the applied voltage, cell viability either remained comparable to the control (0 Hz) or significantly increased, as observed at 500 mV ($p = 0.005$) and 750 mV ($p = 0.041$).

3.2 | Alkaline Phosphatase (ALP) Activity

ALP activity in MC3T3-E1 cells exposed to AC electrostimulation was evaluated at different time points (days 4, 7, 10, and 14) under a range of voltages (125–1500 mV) and frequencies (1, 10, 100, and 1 kHz). An osteogenic control without stimulation was included as reference (Figure 3). Three biological replicates in two independent experiments were analyzed for each day of the study in each defined voltage and frequency.

A clear frequency-dependent pattern was observed across all conditions. High-frequency stimulation (100 Hz and 1 kHz) induced only modest changes or even decreases in ALP activity, with 1 kHz consistently associated with significant decreases over time compared with the control. Conversely, stimulation at 1 Hz resulted in stable values, with no significant variations throughout the experimental period.

The most consistent and robust increases in ALP activity were obtained under 10 Hz stimulation, nevertheless of the applied voltage. At lower voltages (125–500 mV), the enhancement was particularly evident, with significantly higher levels than the osteogenic control at days 10 and 14. At higher voltages (750–1500 mV), the same trend was maintained, albeit with slightly lower magnitudes of response, reinforcing the reproducibility of this effect.

These findings demonstrate that 10 Hz stimulation promotes a sustained enhancement of ALP activity in MC3T3-E1 cells, whereas high-frequency conditions are less effective or even inhibitory. Furthermore, the 10 Hz frequency produced the best results without relying on the highest amplitudes, thus avoiding possible, although unlikely, unwanted harmful effects produced using higher voltages. Considering these results alongside the viability data, 10 Hz was selected as the optimal condition for subsequent experiments, as it combined high cell survival with a significant promotion of early osteoblastic differentiation. As we expected, it was observed a progressive increase in ALP activity throughout the study period at 10 Hz, as this enzyme serves as a hallmark marker of osteoblastic differentiation, reflecting the maturation of pre-osteoblasts into a functional, matrix-secreting phenotype.

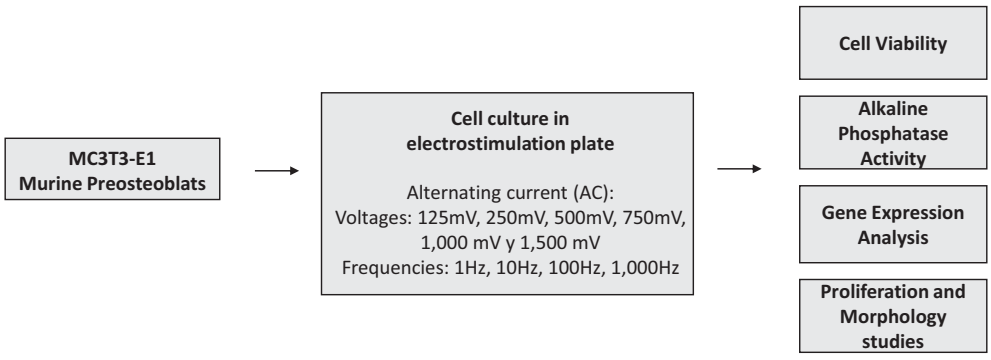

FIGURE 1 | Experimental procedures. Summary.

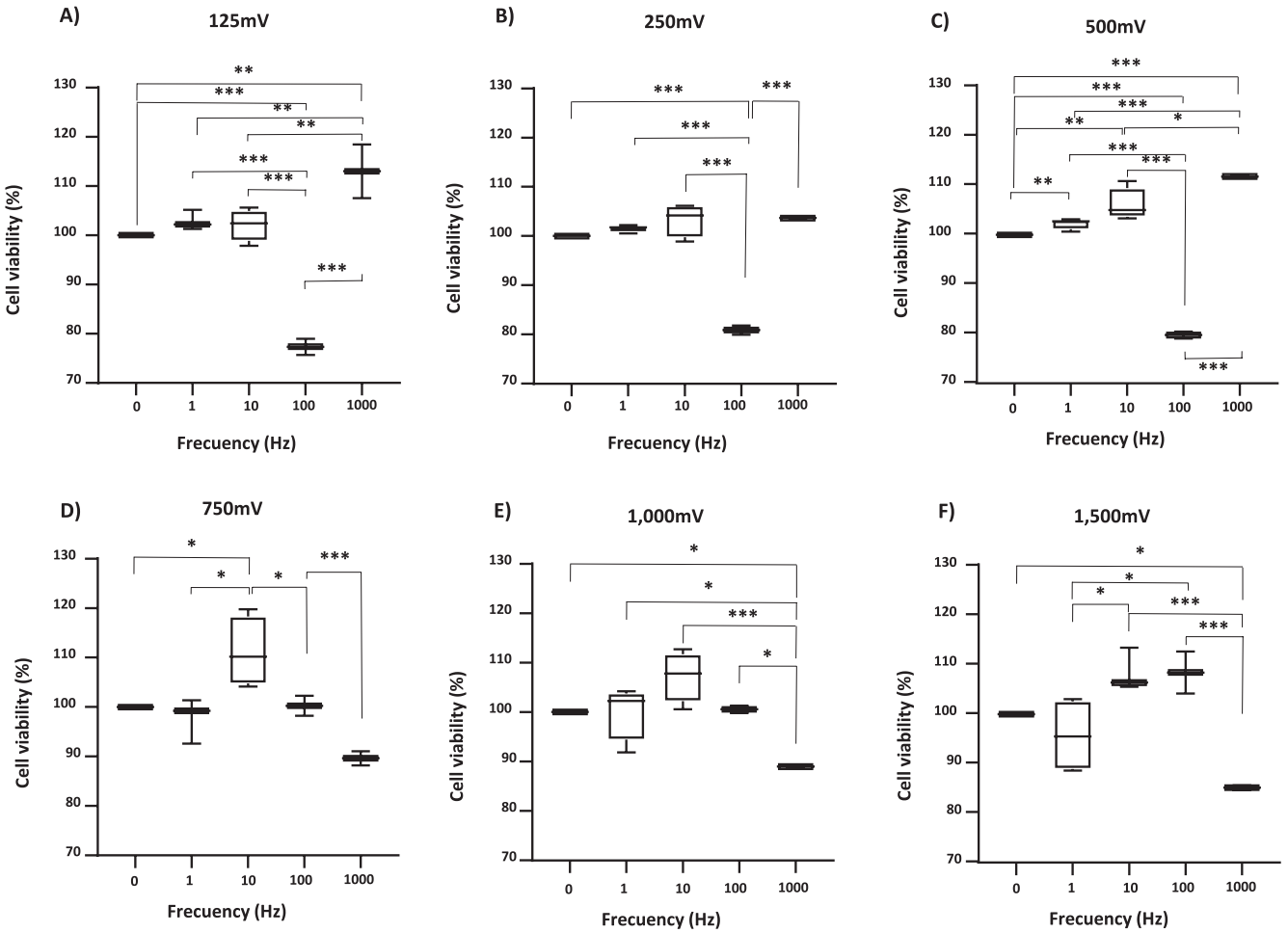

FIGURE 2 | Effect on MC3T3-E1 cell viability applying alternating current (AC) stimulation after 14 days of culture. Cell responses were assessed at frequencies of 0, 1, 10, 100, and 1000 Hz under different voltages: 125 mV (A), 250 mV (B), 500 mV (C), 750 mV (D), 1000 mV (E), and 1500 mV (F). Values are expressed as percentage of viability relative to the unstimulated control (0 Hz). Statistical differences: ***$p < 0.001$; **$p < 0.01$; *$p < 0.05$.

3.3 | Gene Expression Analysis

To determine the effects of alternating current electrical stimulation on the expression of genes involved in osteoblastic differentiation, maturation, and osteogenic activity, we evaluated the transcriptional response of *RUNX2*, *OSX*, *ALP*, *OPG*, and *RANKL* at 10 Hz.

3.3.1 | Osteoblastic Differentiation Gene Analysis

In preosteoblastic MC3T3-E1 cells (Figure 4A–C), low-to-moderate stimulation intensities (125–750 mV) did not significantly alter *RUNX2* expression, although a voltage-dependent upward tendency was observed. In contrast, high-intensity stimulation (1000 and 1500 mV) significantly repressed *RUNX2* transcription, with reductions of 20.00% ± 0.009 and 15.25% ± 0.04, respectively.

A similar pattern was detected for *OSX*. Stimulation between 125 and 750 mV did not induce significant changes, although expression levels tended to increase. However, higher voltages (1000 and 1500 mV) evidently reduced *OSX* expression to 0.37-fold ±0.11 ($p < 0.05$) and 0.37-fold ±0.07 ($p < 0.05$) relative to non-stimulated controls. Statistically significant differences were found between high-voltage conditions and the 250–750 mV range.

As it was shown before, AC stimulation enhanced ALP enzymatic activity, so the study of *ALP* gene expression was necessary. Low and intermediate voltages (125–500 mV) did not produce significant changes, although a consistent upward trend was noted. At 750 mV, *ALP* expression increased significantly (0.76-fold ±0.30, $p = 0.021$), indicating that cells were likely undergoing intermediate stages of differentiation. Conversely, stimulation at 1000 and 1500 mV suppressed *ALP* expression to 0.33-fold ±0.067 ($p < 0.05$) and 0.24-fold ±0.06 ($p < 0.05$), respectively, suggesting that high voltages exert an inhibitory effect on osteoblast maturation.

3.3.2 | Osteoblastic Activity Gene Analysis

To further knowledge about the osteogenic activity of the cells, we evaluated the expression of *OPG* and *RANKL*, two key regulators of the osteoblast–osteoclast function.

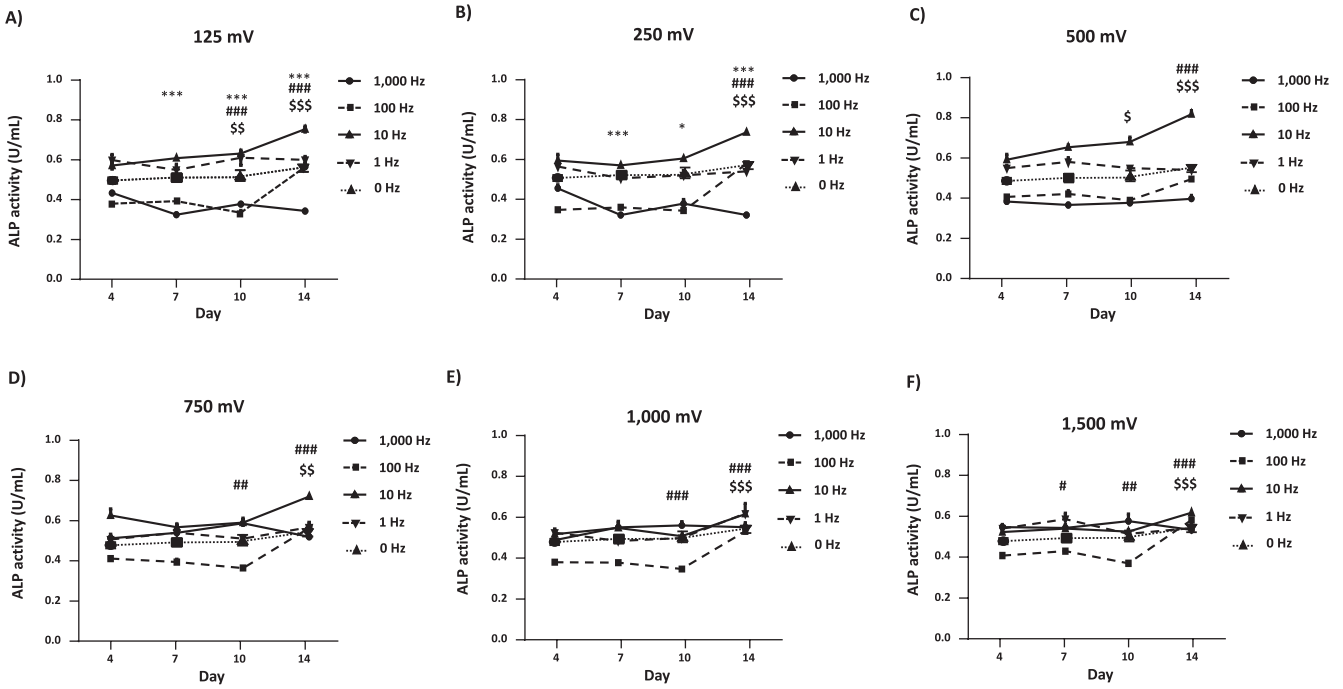

FIGURE 3 | Alkaline phosphatase (ALP) activity in MC3T3-E1 cells subjected to alternating current (AC) stimulation for 4, 7, 10, and 14 days. Frequencies of 0, 1, 10, 100, and 1000 Hz were tested under different voltages: (A) 125 mV, (B) 250 mV, (C) 500 mV, (D) 750 mV, (E) 1000 mV, and (F) 1500 mV. Data are expressed as U/mL and statistical comparison with the unstimulated osteogenic control (0 Hz) in the day of the study. Statistical differences: ***$p < 0.001$; **$p < 0.01$; *$p < 0.05$. (*1000 Hz; # 100 Hz; $ 10 Hz).

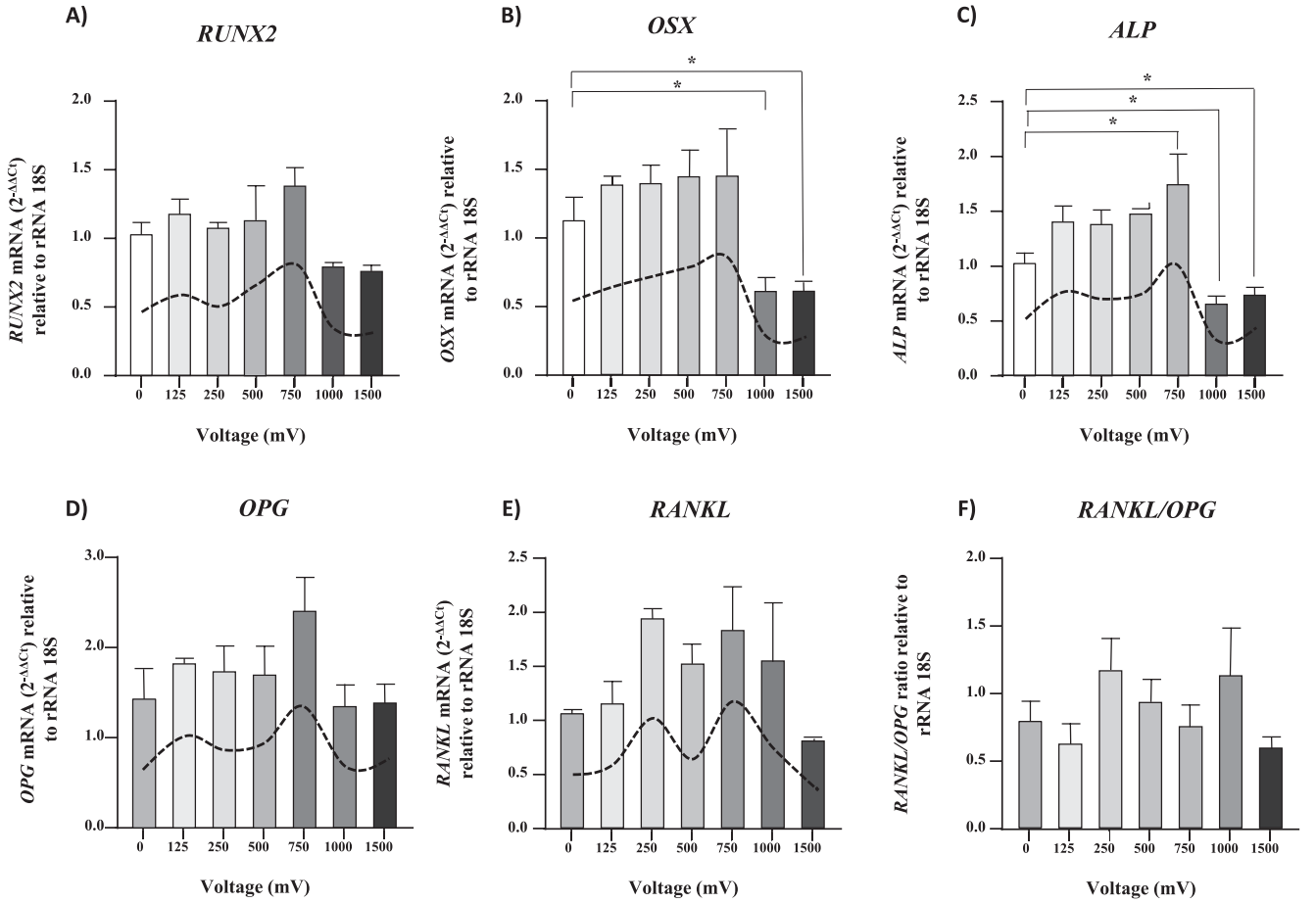

FIGURE 4 | Gene expression in MC3T3-E1 cells after 14 days of AC stimulation (10 Hz; 125–1500 mV) versus cells without electrostimulation (0 mV). *$p < 0.05$. (A) RUNX2 expression; (B) OSX expression; (C) ALP expression; (D) OPG expression; (E) RANKL expression; (F) RANKL/OPG ratio.

For *OPG*, (Figure 4D–F), no significant differences were detected across the stimulation conditions. However, a voltage-dependent tendency toward upregulation was observed between 125 and 750 mV, similar to the pattern previously well known for *RUNX2*, *OSX*, and *ALP*. At higher voltages (1000 and 1500 mV), *OPG* expression declined. In contrast, *RANKL* expression remained largely unaffected by AC stimulation, with no significant differences between stimulated and control groups. Consequently, the RANKL/OPG ratio, an indicator of resorptive versus osteogenic activity, did not differ significantly under any of the tested conditions, suggesting that AC stimulation did not alter the osteoblastic–osteoclastic balance in MC3T3-E1 cells.

3.4 | Cell Proliferation Counting

MC3T3-E1 cells nuclei quantification across 40 random fields revealed a voltage-dependent proliferative response. Significant increases were observed at 125 mV (52.86% ± 2.95, $p < 0.001$), 250 mV (55.13% ± 2.40, $p < 0.001$), and 500 mV (69.62% ± 3.52, $p < 0.001$). At 750 mV, proliferation also increased significantly, though to a lesser extent (34.92% ± 5.95, $p = 0.017$). In contrast, higher voltages (1000 and 1500 mV) did not produce significant differences compared to non-stimulated controls (Figure 5).

3.5 | Morphometric and Cell Differentiation Analysis

Cell morphology was analyzed in mCherry+ MC3T3-E1 cells subjected to AC stimulation at 10 Hz during 14 days with different voltages. Quantification of cell area revealed significant reductions only at high voltages, with values of 41.71 ± 11.43 μm^2 at 1000 mV and 37.89 ± 11.58 μm^2 at 1500 mV, compared with 86.78 ± 24.61 μm^2 in controls ($p < 0.001$). At lower voltages (125–750 mV), no decreases were observed. Remarkably, 500 mV induced a significantly superior area (99.06 ± 5.05 μm^2) compared with 77.64 ± 3.03 μm^2 at 750 mV ($p = 0.036$), indicating a favorable condition for cell spreading.

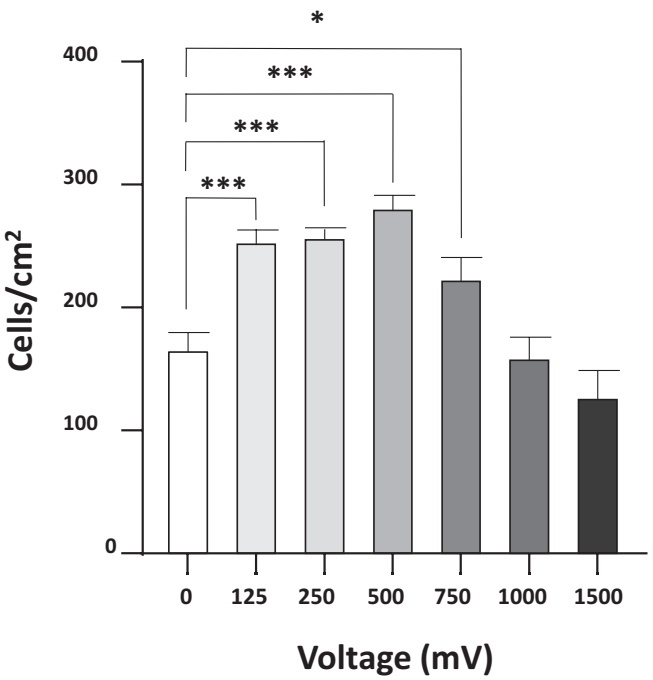

FIGURE 5 | MC3T3-E1 cell proliferation after 14 days of AC stimulation at 10 Hz with voltages of 125, 250, 500, 750, 1000, and 1500 mV. 40 random fields were analyzed in each defined voltage at 10 Hz. (*$p < 0.05$; **$p < 0.01$; ***$p < 0.001$).

The mean number of pseudophilopodia per cell remained unchanged across all conditions, averaging 3.51 ± 0.34 pseudopodia/cell, suggesting that AC stimulation neither promoted the formation of new extensions nor induced retraction of existing ones.

In contrast, pseudophilopodia length showed voltage-dependent modulation. Mean length progressively increased up to 500 mV (14.28 ± 4.97 μm vs. 7.44 ± 3.08 μm in controls, $p < 0.001$), with 250 mV also producing a significant effect (12.28 ± 1.17 μm, $p = 0.017$). Maximal pseudophilopodia length was significantly extended only at 500 mV (19.88 ± 6.02 μm vs. 13.27 ± 5.49 μm in controls, $p = 0.0053$) (Figure 6).

Taken together, 500 mV produced the strongest enhancement of proliferation, cell area, and pseudophilopodia elongation, whereas 750 mV was the only condition associated with significant overexpression of ALP, consistent with osteoblastic maturation. These observations identified 10 Hz and 500–750 mV as the most favorable conditions to induce an earlier osteoblastic differentiation.

4 | Discussion

Electrostimulation has emerged as a promising technique in the field of bioengineering and biomedicine, particularly in bone regeneration and cell differentiation in terms of an induction of the early osteogenic phenotype. The objective of this study was to evaluate the effects of different ES conditions on the cellular viability and osteoblastic differentiation of the MC3T3-E1 cell line. This analysis focuses on evaluating how changes in ES frequency and voltage amplitude of squared biphasic ES signals impact osteoblastic cell proliferation, differentiation, and morphology.

A notable feature of this experimental setup is the electrode configuration, which has allowed the cells in culture to grow on top of the electrodes and be influenced by the complete applied electrical potential generated. In turn, it was possible to determine the direction of this electric field because ionic charge moved from the anode to cathode [22].

ES was applied for 14 days with the objective of accelerating osteogenic differentiation. The duration of stimulation is an essential parameter for clinical application, as highlighted by Wang and colleagues [9]. Prolonged exposure to 50 Hz can induce DNA damage and reduce cell viability [23]. Therefore, the stimulus time is fundamental for optimizing ES protocols.

Parameters such as frequency and voltage are critical. Frequencies outside the 10–1000 Hz range do not promote cell proliferation [24]. Mahadeo and colleagues [25] also used 10 Hz, since higher frequencies degraded RNA and the electrodes. Our

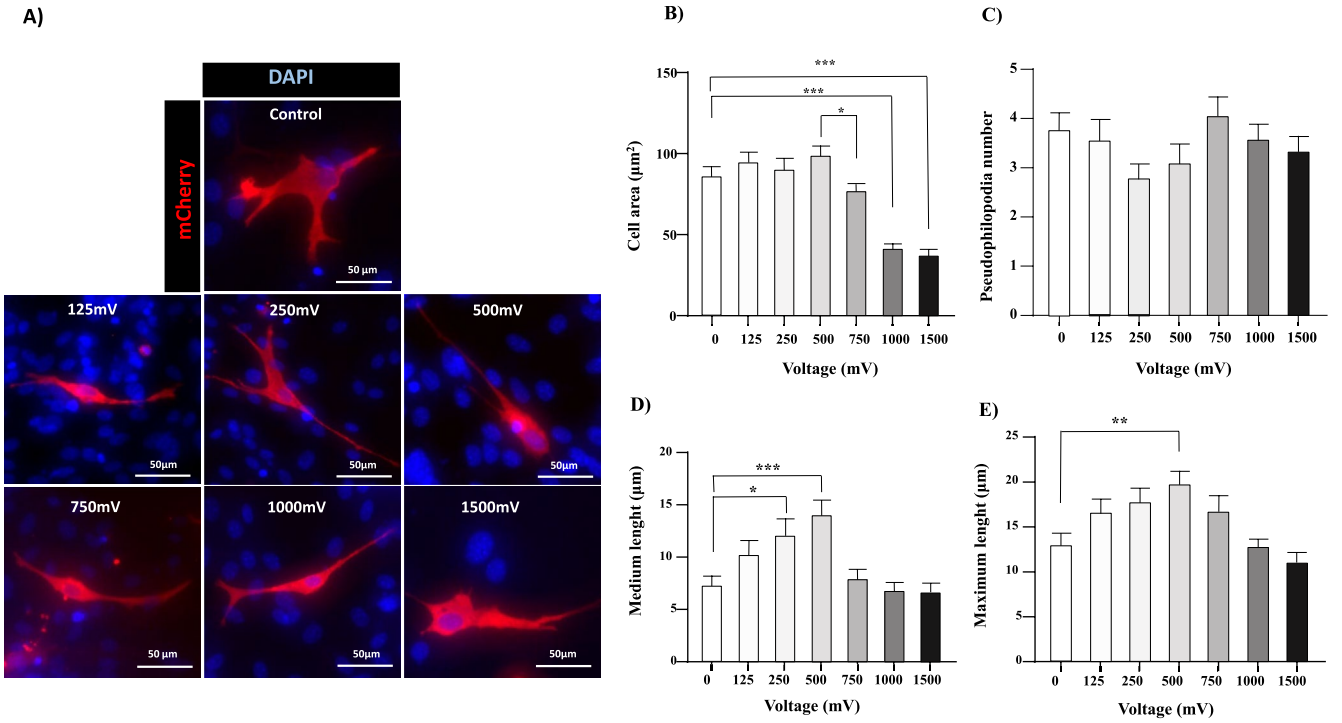

FIGURE 6 | Immunofluorescence of MC3T3-E1 cells after 14 days of AC stimulation at 10 Hz with voltages of 125, 250, 500, 750, 1000, and 1500 mV compared to control (0 mV). (**A**) Red (mCherry) indicates cells transfected with the mCherry plasmid, and blue (DAPI) marks cell nuclei. (B) Cell area (μm^2). (C) Number of pseudophilopodia. (D) Mean pseudophilopodia length. (E) Maximum pseudophilopodia length. All measurements were performed in MC3T3-E1 cells after 14 days of AC stimulation at 10 Hz under the indicated voltages compared to control (0 mV). 40 transfected cells were analyzed for each day of the study in each defined voltage at 10 Hz. (*$p < 0.05$; **$p < 0.01$; ***$p < 0.001$).

data show that the MC3T3-E1 cells reached maximum viability and proliferation at 10 Hz with 500 and 750 mV/mm. In contrast, higher voltages and frequencies decrease cell viability, suggesting cytotoxic effects [25]. Therefore, 10 Hz frequency is considered safe and effective, being in concordance with previous studies [24].

Cell viability results are consistent with ALP activity. The highest enzymatic ALP activity in MC3T3 was observed at 10 Hz with 500 and 750 mV/mm, supporting findings from Wang et al. [9]. These results emphasize the importance of carefully adjusting frequency and voltage to avoid ion accumulation, ROS generation, or abrupt pH changes that may damage DNA [23].

At the genetic level, ES induced osteoblastic early differentiation and osteogenic activity by increasing the expression of *RUNX2*, *OSX*, *ALP*, and *OPG* at 10 Hz with 500 and 750 mV/mm, consistent with Sahm et al. 2020 [26].

Regarding the gene expression profile, it is important to note that while *ALP* showed a significant upregulation under optimized AC stimulation (10 Hz, 750 mV/mm) at day 14, no significant differences were observed for *RUNX2* and *OSX* at this time point. This observation is likely attributable to the temporal dynamics of osteogenic markers; *RUNX2* and *OSX* are key early-stage transcription factors whose expression typically peaks during the initial phases of pre-osteoblast proliferation. By day 14, the culture has progressed toward matrix maturation, a stage where ALP activity is more prominent, being an essential marker of differentiation, as evidenced by our results. Therefore, the lack of significant changes in *RUNX2* and *OSX* at day 14 does not necessarily imply a lack of stimulus-induced differentiation, but rather suggests that the evaluation was performed beyond their transitory peak expression. These findings highlight the importance of the stimulation window and suggest that AC parameters effectively enhance early differentiation, as confirmed by the sustained increase in *ALP* expression.

Although a limitation of this study is that the opaque gold-electrode substrate of the 8W10E+ chambers may interfere with colorimetric quantification required for mineralization assays. Moreover, our electrostimulation protocol was validated up to 14 days, and potential effects of prolonged culture (21–28 days), including electrode stability and byproduct accumulation, were not assessed. Future work should incorporate mineralization assays (Alizarin Red, von Kossa), calcium deposition quantification, and mature osteoblast markers such as osteocalcin protein expression, ideally using transparent-bottom chambers and protocols specifically designed to evaluate electrode functionality over extended periods.

Other studies as Wang et al. [9], identified frequency as a dominant factor, showing that 10–100 Hz overexpress genes such as *RUNX2* and *ALP*. In our study, *OSX* and *ALP* were repressed at higher voltages (1000 and 1500 mV/mm) and at 10 Hz, while *ALP* was induced at 750 mV/mm. These effects could be mediated by the BMP-2 signaling pathway via Smad1/5/8, which promotes *RUNX2* expression [27]. Other studies have also demonstrated that ES induces genes such as *RUNX*, *ALP*, and *OCN* in MG-63 osteosarcoma and Saos-2 cells [10, 28].

This study analyses in this electrostimulation setup the effect of electrostimulation conditions on the expression of *RANKL* and *OPG* genes in MC3T3-E1 cells. *OPG* was overexpressed at 10 Hz and 750 mV/mm. Furthermore, while *RANKL* expression and the *RANKL/OPG* ratio did not show statistically significant changes, a discernible trend in the direction of an osteogenic balance. This tendency of decreasing favors bone formation, similar to what is observed with electromagnetic fields [29], which suggests that ES could modulate bone remodeling too.

At the morphological level, ES increased pseudophilopodia length at 500 mV/mm, whereas higher voltages reduced cell area, suggesting a negative effect [30]. Optimal voltages promoted the elongation of pseudophilopodia. Enhancing adhesion and chemotaxis, processes that depend on morphology [31, 32]. ES also modifies the expression profile of membrane proteins such as integrins [33] and vinculin [34]. This could be explained by galvanotaxis, where the negative membrane potential guides cell migration [35, 36].

In summary, this study demonstrates that ES is a promising strategy to promote osteogenesis. While we acknowledge that the effects of AC on osteoblasts have been previously explored [37–39], the novelty of our work is based on the systematic optimization of specific frequency and voltage parameters (10 Hz, 750 mV/mm) within our unique experimental setup. Taking that item into account, this study provides a comprehensive characterization of how AC frequency and voltage parameters jointly influence proliferation, viability, early differentiation, and morphology in MC3T3-E1 cells using this electrostimulation system. The optimization of stimulation parameters—especially duration, frequency and voltage—is essential. Notably, ES at 10 Hz and 750 mV/mm induced cell proliferation, early differentiation, and favorable morphological changes in MC3T3-E1 cells, highlighting it as a promising advance in regenerative medicine.

Author Contributions

Conceptualization: Mercè Giner, Alberto Yufera and Mª José Montoya-García. Methodology: Jesús Bocio-Núñez, Daniel Martín and Pedro J. Chacón. Formal analysis and investigation: Jesús Bocio-Núñez and Mercè Giner. Writing – original draft preparation: Jesús Bocio-Núñez, Daniel Martín and Pedro J. Chacón; Writing – review and editing: Mercè Giner, Alberto Yufera and Mª José Montoya-García; Funding acquisition: Alberto Yufera; Resources: Miguel Ángel Rico, Miguel Ángel Colmenero and Mª José Montoya-García; Supervision: Mercè Giner and Alberto Yufera. All authors commented, read, and approved the final manuscript.

Acknowledgments

This research was supported for R&D&I projects within the framework of the FEDER Andalusia 2014-2020 Operational Programme. Project Title: Medicine and Electrostimulation System for Cell Differentiation Applications.

Funding

This work was supported by the Andalusian Government, P18-FR-2038, Regional Ministry of Economy and Knowledge of Junta de Andaluc&ía, the I+D+i Program (Proyectos de Excelencia). Open Access funding provided thanks to the CRUE-CSIC agreement with Wiley.

Conflicts of Interest

The authors declare no conflicts of interest.

Data Availability Statement

All raw data are shown alongside the article. There are no data to be shared in association with this manuscript; therefore, no data are made available.

References

1. C. Chen, X. Bai, Y. Ding, and I. S. Lee, "Electrical Stimulation as a Novel Tool for Regulating Cell Behavior in Tissue Engineering," *Biomaterials Research* 23 (2019): 25.

2. Y. Yuste, J. A. Serrano, A. Olmo, et al., *Monitoring Muscle Stem Cell Cultures With Impedance Spectroscopy, in BIODEVICES 2018: 11th International Joint Conference on Biomedical Engineering Systems and Technologies* (ScitePress Digital Library, 2018), 96–99.

3. S. B. Rajendran, K. Challen, K. L. Wright, and J. G. Hardy, "Electrical Stimulation to Enhance Wound Healing," *Journal of Functional Biomaterials* 12 (2021): 40.

4. L. Juckett, T. M. Saffari, B. Ormseth, J. L. Senger, and A. M. Moore, "The Effect of Electrical Stimulation on Nerve Regeneration Following Peripheral Nerve Injury," *Biomolecules* 12 (2022): 1856.

5. B. Mollon, V. da Silva, J. W. Busse, T. A. Einhorn, and M. Bhandari, "Electrical Stimulation for Long-Bone Fracture-Healing: A Meta-Analysis of Randomized Controlled Trials," *Journal of Bone and Joint Surgery-American Volume* 90 (2008): 2322–2330.

6. C. P. Huang, X. M. Chen, and Z. Q. Chen, "Osteocyte: The Impresario in the Electrical Stimulation for Bone Fracture Healing," *Medical Hypotheses* 70 (2008): 287–290.

7. T. deVet, A. Jhirad, L. Pravato, and G. R. Wohl, "Bone Bioelectricity and Bone-Cell Response to Electrical Stimulation: A Review," *Critical Reviews in Biomedical Engineering* 49 (2021): 1–19.

8. E. Pettersen, F. A. Shah, and M. Ortiz-Catalan, "Enhancing Osteoblast Survival Through Pulsed Electrical Stimulation and Implications for Osseointegration," *Scientific Reports* 11 (2021): 22416.

9. Y. Wang, H. Cui, Z. Wu, et al., "Modulation of Osteogenesis in MC3T3-E1 Cells by Different Frequency Electrical Stimulation," *PLoS One* 11 (2016): e0154924.

10. S. Meng, M. Rouabhia, and Z. Zhang, "Electrical Stimulation Modulates Osteoblast Proliferation and Bone Protein Production Through Heparin-Bioactivated Conductive Scaffolds," *Bioelectromagnetics* 34 (2013): 189–199.

11. H. M. Kronenberg, "Developmental Regulation of the Growth Plate," *Nature* 423 (2003): 332–336.

12. I. Corre, F. Verrecchia, V. Crenn, F. Redini, and V. Trichet, "The Osteosarcoma Microenvironment: A Complex but Targetable Ecosystem," *Cells* 9 (2020): 976.

13. W. Liu, S. Toyosawa, T. Furuichi, et al., "Overexpression of Cbfa1 in Bone and Tooth Research," *Official Journal of the American Society for Bone and Mineral Research* 16 (2001): 1957–1966.

14. R. Nishimura, M. Wakabayashi, K. Hata, et al., "Osterix Regulates Calcification and Degradation of Chondrogenic Matrices Through Matrix Metalloproteinase 13 (MMP13) Expression in Association With Transcription Factor Runx2 During Endochondral Ossification," *Journal of Biological Chemistry* 287 (2012): 33179–33190.

15. W. C. W. Chan, Z. Tan, M. K. T. To, and D. Chan, "Regulation and Role of Transcription Factors in Osteogenesis," *International Journal of Molecular Sciences* 22 (2021): 5445.

16. W. Huang, S. Yang, J. Shao, and Y. P. Li, "Signaling and Transcriptional Regulation in Osteoblast Commitment and Differentiation," *Frontiers in Bioscience: A Journal and Virtual Library* 12 (2007): 3068–3092.

17. D. S. Amarasekara, S. Kim, and J. Rho, "Regulation of Osteoblast Differentiation by Cytokine Networks," *International Journal of Molecular Sciences* 22 (2021): 2851.

18. X. Chen, X. Zhi, J. Wang, and J. Su, "RANKL Signaling in Bone Marrow Mesenchymal Stem Cells Negatively Regulates Osteoblastic Bone Formation," *Bone Research* 6 (2018): 34.

19. A. G. Robling and L. F. Bonewald, "The Osteocyte: New Insights," *Annual Review of Physiology* 82 (2020): 485–506.

20. C. Greenhill, "Osteoprotegerin Sources Examined," *Nature Reviews. Endocrinology* 16 (2020): 678.

21. D. Martín, D. Ruano, A. Yúfera, and P. Daza, "Electrical Pulse Stimulation Parameters Modulate N2a Neuronal Differentiation," *Cell Death Discovery* 10 (2024): 49.

22. D. Martin, J. Bocio-Nuñez, S. F. Scagliusi, et al., "DC Electrical Stimulation Enhances Proliferation and Differentiation on N2a and MC3T3 Cell Lines," *Journal of Biological Engineering* 16 (2022): 27.

23. F. I. Wolf, A. Torsello, B. Tedesco, et al., "50-Hz Extremely Low Frequency Electromagnetic Fields Enhance Cell Proliferation and DNA Damage: Possible Involvement of a Redox Mechanism," *Biochimica et Biophysica Acta* 1743 (2005): 120–129.

24. C. Wennberg, L. Hessle, P. Lundberg, et al., "Functional Characterization of Osteoblasts and Osteoclasts From Alkaline Phosphatase Knockout Mice," *Journal of Bone and Mineral Research: The Official Journal of the American Society for Bone and Mineral Research* 15 (2000): 1879–1888.

25. C. O. Mahadeo, A. Shahin-Shamsabadi, M. Khodamoradi, M. Fahnestock, and P. R. Selvaganapathy, "The Effects of Electrical Stimulation on a 3D Osteoblast Cell Model," *Cells* 14 (2025): 396.

26. F. Sahm, J. Ziebart, A. Jonitz-Heincke, D. Hansmann, T. Dauben, and R. Bader, "Alternating Electric Fields Modify the Function of Human Osteoblasts Growing on and in the Surroundings of Titanium Electrodes," *International Journal of Molecular Sciences* 21 (2020): 6944.

27. X. Liu, F. Cao, S. Liu, Y. Mi, and J. Liu, "BMP2/Smad Signaling Pathway Is Involved in the Inhibition Function of Fibroblast Growth Factor 21 on Vascular Calcification," *Biochemical and Biophysical Research Communications* 503 (2018): 930–937.

28. R. A. Gittens, R. Olivares-Navarrete, R. Rettew, et al., "Electrical Polarization of Titanium Surfaces for the Enhancement of Osteoblast Differentiation," *Bioelectromagnetics* 34 (2013): 599–612.

29. A. Catalano, S. Loddo, F. Bellone, C. Pecora, A. Lasco, and N. Morabito, "Pulsed Electromagnetic Fields Modulate Bone Metabolism via RANKL/OPG and Wnt/β-Catenin Pathways in Women With Postmenopausal Osteoporosis: A Pilot Study," *Bone* 116 (2018): 42–46.

30. N. Ozkucur, T. K. Monsees, S. Perike, H. Q. Do, and R. H. Funk, "Local Calcium Elevation and Cell Elongation Initiate Guided Motility in Electrically Stimulated Osteoblast-Like Cells," *PLoS One* 4 (2009): e6131.

31. S. Staehlke, M. Bielfeldt, J. Zimmermann, et al., "Pulsed Electrical Stimulation Affects Osteoblast Adhesion and Calcium Ion Signaling," *Cells* 11 (2022): 2650.

32. R. Balint, N. J. Cassidy, and S. H. Cartmell, "Electrical Stimulation: A Novel Tool for Tissue Engineering," *Tissue Engineering, Part B, Reviews* 19 (2013): 48–57.

33. I. S. Aleem, I. Aleem, N. Evaniew, et al., "Efficacy of Electrical Stimulators for Bone Healing: A Meta-Analysis of Randomized Sham-Controlled Trials," *Scientific Reports* 6 (2016): 31724.

34. A. Kumar, M. Ouyang, K. van den Dries, et al., "Talin Tension Sensor Reveals Novel Features of Focal Adhesion Force Transmission and Mechanosensitivity," *Journal of Cell Biology* 213 (2016): 371–383.

35. R. L. Duncan and C. H. Turner, "Mechanotransduction and the Functional Response of Bone to Mechanical Strain," *Calcified Tissue International* 57 (1995): 344–358.

36. B. M. Isaacson and R. D. Bloebaum, "Bone Bioelectricity: What Have We Learned in the Past 160 Years?," *Journal of Biomedical Materials Research. Part A* 95 (2010): 1270–1279.

37. J. H. Jansen, O. P. van der Jagt, B. J. Punt, et al., "Stimulation of Osteogenic Differentiation in Human Osteoprogenitor Cells by Pulsed Electromagnetic Fields: An in Vitro Study," *BMC Musculoskeletal Disorders* 11 (2010): 188.

38. F. Sahm, A. Jakovljevic, R. Bader, R. Detsch, and A. Jonitz-Heincke, "Is There an Influence of Electrically Stimulated Osteoblasts on the Induction of Osteoclastogenesis?," *Applied Sciences* 12 (2022): 11840.

39. B. Hiemer, J. Ziebart, A. Jonitz-Heincke, et al., "Magnetically Induced Electrostimulation of Human Osteoblasts Results in Enhanced Cell Viability and Osteogenic Differentiation," *International Journal of Molecular Medicine* Jul 1 38, no. 1 (2016): 57–64.

Supporting Information

Additional supporting information can be found online in the Supporting Information section. **Table S1:** Primers used in real time quantitative PCR experiments, including name of oligonucleotide, reference or sequence (5′–3′), specie and product size (pb).